Available online at www.sciencedirect.com

ScienceDirect

Biochimica et Biophysica Acta 1778 (2008) 907–916

Biochimica et Biophysica Acta BBA

www.elsevier.com/locate/bbamem

Influence of salt on the structure of DMPG studied by SAXS and optical microscopy

Roberto M. Fernandez *,[1], Karin A. Riske [2], Lia Q. Amaral, Rosangela Itri, M. Teresa Lamy

Instituto de Física da Universidade de São Paulo, CP 66.318 CEP 05315-970, São Paulo, SP, Brazil

Received 11 July 2007; received in revised form 5 December 2007; accepted 7 December 2007
Available online 15 December 2007

Abstract

Aqueous dispersions of 50 mM dimyristoylphosphatidylglycerol (DMPG) in the presence of increasing salt concentrations (2–500 mM NaCl) were studied by small angle X-ray scattering (SAXS) and optical microscopy between 15 and 35 °C. SAXS data show the presence of a broad peak around $q \sim 0.12$ Å^{-1} at all temperatures and conditions, arising from the electron density contrasts within the bilayer. Up to 100 mM NaCl, this broad peak is the main feature observed in the gel and fluid phases. At higher ionic strength (250–500 mM NaCl), an incipient lamellar repeat distance around $d = 90$–100 Å is detected superimposed to the bilayer form factor. The data with high salt were fit and showed that the emergent Bragg peak is due to loose multilamellar structures, with the local order vanishing after $\sim 4d$. Optical microscopy revealed that up to 20 mM NaCl, DMPG is arranged in submicroscopic vesicles. Giant (loose) multilamellar vesicles (MLVs) start to appear with 50 mM NaCl, although most lipids are arranged in small vesicles. As the ionic strength increases, more and denser MLVs are seen, up to 500 mM NaCl, when MLVs are the prevailing structure. The DLVO theory could account for the experimentally found interbilayer distances.

Keywords: Gel–fluid phase transition; Intermediate phase; Charged phospholipid; DLVO theory

1. Introduction

Most cells and organisms bear a net negative charge on their membrane surface. Because of that, charged lipids have been widely studied, although most of the extensive characterization of bilayer properties has been carried out with neutral lipids, mainly with phosphatidylcholines [1]. Phosphatidylglycerols are the most abundant anionic lipids found in prokaryotes and have been extensively used as a model for negatively charged membranes [2–5], one of the reasons being that they show, under physiological conditions, quite similar properties to those found with phosphatidylcholines bearing the same acyl chains. One key difference between charged and uncharged lipids is the amount of water stabilized between bilayers. Neutral lipids like PCs spontaneously form multilamellar structures with a definite water layer among them, defined by a balance between van der Waals attraction and repulsive hydration and steric forces [6]. These multilamellar structures can be either a true lamellar phase for low water content or multilamellar vesicles (MLVs) at lower lipid concentrations (for a comprehensive review on lecithin bilayer structure, see [1] and references therein). On the other hand, charged lipids at low ionic strength usually form fully hydrated unilamellar vesicles [7–9], as the charges add a long range repulsive interaction. Addition of high enough salt concentrations, however, can lead to balance of repulsive and attractive interactions, and thus multilamellar structures can be formed, as observed, for example, with dipalmitoylphosphatidylglycerol [10]. The study of the properties of charged lipids in the presence of electrolytes is of great biological relevance, as it can help elucidate the physical aspects underlying many important biological events.

In this work, we study the structures spontaneously formed by dimyristoylphosphatidylglycerol (DMPG) when dispersed in

* Corresponding author. Tel./fax: +55 14 3811 6254.
E-mail address: rmorato@ibb.unesp.br (R.M. Fernandez).
[1] Present address: Depto. de Física e Biofísica, Instituto de Biociências da Universidade Estadual Paulista, CP 510 CEP 18618-000, Botucatu, SP, Brazil.
[2] Present address: Depto. Biofísica da Universidade Federal de São Paulo, R. Botucatu, 862 CEP 04023-062 São Paulo, SP, Brazil.

0005-2736/$ - see front matter © 2007 Elsevier B.V. All rights reserved.
doi:10.1016/j.bbamem.2007.12.005

a buffer solution at different salt concentrations. It has been shown previously, that DMPG at low ionic strength and neutral pH presents an extended gel–fluid transition region, called the intermediate phase (IP), between the well-known gel and fluid phases [3,11–14]. This phase shows some features not found in its neighboring phases: an unusually low turbidity [3,12], high conductivity [12] and high viscosity [3,15]. Small angle X-ray scattering (SAXS) performed on low ionic strength dispersions (50 mM DMPG in 10 mM Hepes+2 mM NaCl) showed the presence of a broad peak around $q=0.12$ Å^{-1}, due to the bilayer form factor at all temperatures [13]. No Bragg diffraction peak, characteristic of multilamellar structures, was detected, evidencing that at low ionic strength DMPG is arranged in uncorrelated bilayers. The SAXS curves could be well-fit by a single bilayer form factor, with bilayer thickness and electron density contrast changing in the different temperature regions [13]. Additional X-ray results extending the low angle region revealed the existence of structures around 400 Å only in the IP, which was interpreted as in-plane correlated cavities/pores on the vesicle surface [16].

As the ionic strength is increased, the temperature extension of the IP is reduced, as seen by DSC, turbidity and spectroscopic techniques with 10 mM DMPG [8,12,15,17]. Around 100–500 mM NaCl, the IP is not detected and the thermal behavior of DMPG resembles that of DMPC (dimyristoylphosphatidylcholine), with a single T_m around 23 °C. A further increase in salt concentration to 2 M NaCl causes an increase in T_m up to 29 °C [18]. A detailed study of the structure of the high salt phase of DMPG was still lacking. In the present work, we investigate the thermal behavior and structure of 50 mM DMPG between 2 and 500 mM NaCl by SAXS and optical microscopy. The latter technique has been widely used to visualize giant unilamellar vesicles [19,20]. We show here that it provides also unique insights in the more general study of lipid dispersions.

2. Materials and methods

2.1. Materials

The sodium salt of the phospholipid DMPG (1,2-dimyristoyl-*sn*-glycero-3-[phospho-*rac*-glycerol]) was purchased from Avanti Polar Lipids (Alabaster, AL, USA). The buffer system was 10 mM Hepes (4-(2-hydroxyethyl)-1-piperizineethanesulfonic acid) adjusted with NaOH to pH 7.4. Milli-Q water was used throughout.

2.2. Lipid dispersion preparation

A lipid film was formed from a chloroform solution of 50 mM DMPG, dried under a stream of N_2 and left under reduced pressure for a minimum of 2 h, to remove all traces of the organic solvent. Dispersions were prepared by the addition of the Hepes buffer with different salt concentrations (from 2 mM up to 500 mM NaCl), followed by vortexing for about 2 min above T_m^{off} (~35 °C). The samples were kept at room temperature and used within some hours after preparation. The reproducibility of the results in connection with the sample preparation procedure will be discussed later.

2.3. Optical microscopy

Dispersions of 50 mM DMPG were prepared at different salt concentrations as described above and then diluted to 2.5 mM DMPG (20 mM NaCl) and 0.7 mM DMPG (50–500 mM NaCl) to reduce sample turbidity and allow for optical imaging. As discussed in the text, structures already formed due to salt effects are not expected to change upon dilution and/or further salt addition in the experiment timescale. The dispersions were observed in an inverted microscope Zeiss Axiovert 200 with a 63× Ph2 objective. Images were obtained with a digital camera Zeiss AxioCam HSm. Both phase contrast and bright field modes were used to visualize the sample. In some cases, the temperature was controlled with a bath circulator Lauda RE-106.

2.4. Small angle X-ray scattering

Most measurements were performed in the SAXS beam line of the LNLS (National Laboratory of Synchrotron Radiation, Campinas, SP, Brazil). The X-ray wavelength used was $\lambda=1.608$ Å, and the SAXS sample detector distance was around 1300 mm. A linear position-sensitive image plate detector was used, with resolution 250–300 μm. Samples with 1 mm thickness were conditioned in a Teflon sample holder with flat Mylar walls. A thermal bath was used for temperature variation in the interval between 15 and 45 °C. Data were normalized for the acquisition time (10 min), monitor integral counts (to compensate for oscillations in the beam intensity), and sample attenuation. A measurement to check the effect of different forms of sample preparation was done at the Rigaku-Denki X-ray generator equipment (Laboratory of Crystallography of the Institute of Physics, University of Sao Paulo) with Cu rotating anode (Cu–K_α radiation wavelength, $\lambda=1.5418$ Å) in linear focus geometry to increase intensity. A sample detector distance of 485 mm was used with a time exposure of 12 h. Samples were conditioned in glass capillary (internal diameter 1.5 mm). The scattering due to the buffer was subtracted from all SAXS curves. The fitting to the experimental curves was done with the Microcal Origin software.

2.5. Step-model for the bilayer form factor

It is well-known that the X-ray scattering intensity in an infinite flat membrane approximation (in this case, the exponent of q is expected to be 2) is given by [21]:

$$I(q)=\frac{N}{q^2}\cdot\left[F(q)^2\right]\cdot S(q) \tag{1}$$

where N is the normalization constant, q is the scattering vector ($q=4\pi\sin(\theta)/\lambda$, with 2θ being the scattering angle), $F(q)$ the form factor and $S(q)$ the interference function.

F(q) is calculated taking the Fourier transform of the electron density $\rho(x)$ of the membrane structure in the direction perpendicular to the bilayer plane and t is the bilayer thickness:

$$F(q)=\int_{-t/2}^{t/2}\rho(x)\cdot\cos(q\cdot x)dx \tag{2}$$

Assuming that the electron density is represented by three different constant values, related to the headgroup, the acyl chains and the methyl group, Eq. (2) can be rewritten in terms of the thickness (R_i) and electron density (ρ_i) parameters of each region, as follows [13]:

$$F(q)=\frac{2}{q}\cdot\{\Delta\rho_3\cdot\sin qR_3+\Delta\rho_2\cdot[\sin q(R_2+R_3)-\sin qR_3]+\Delta\rho_1\cdot[\sin q(R_1+R_2+R_3)-\sin q(R_2+R_3)]\} \tag{3}$$

where $\Delta\rho_i$ is the electron density difference between ρ_i and the solvent (ρ_w). The indexes 1, 2, and 3 refer to the headgroup, acyl chain and methyl group regions, respectively.

3. Results and discussion

3.1. Small angle X-ray scattering data

SAXS measurements were performed with 50 mM DMPG in the presence of 2–500 mM NaCl) between 15 and 35 °C. Fig. 1

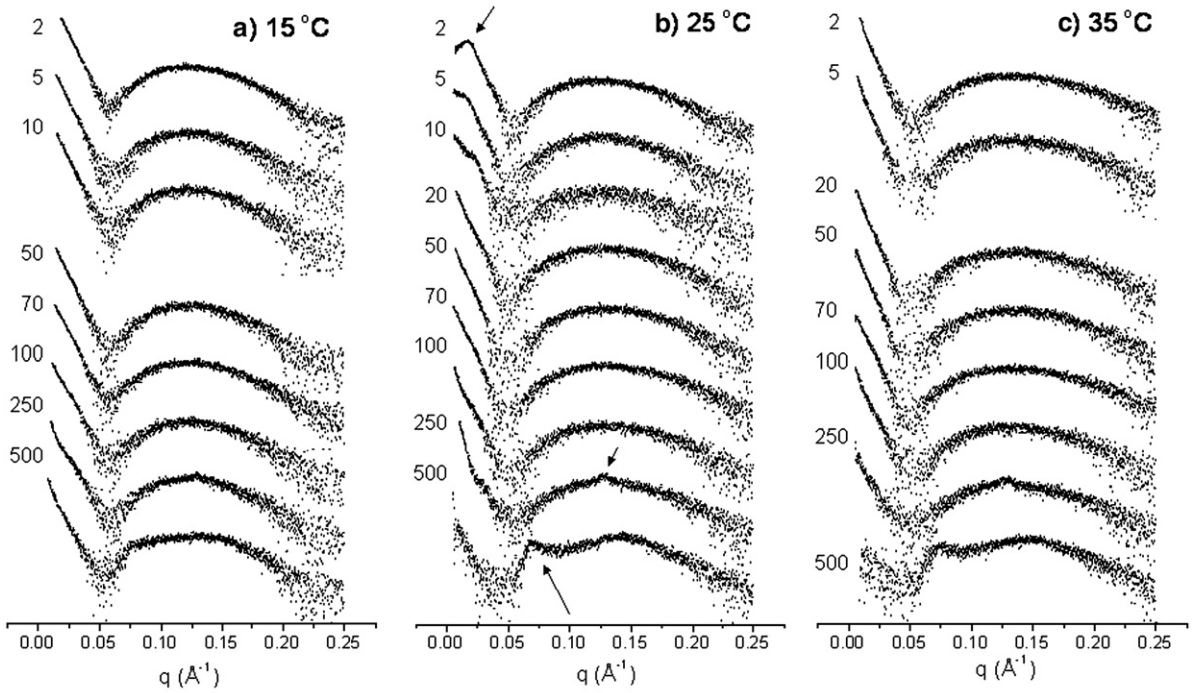

Fig. 1. SAXS curves of 50 mM DMPG in 10 mM Hepes pH 7.5 at a) 15, b) 25 and c) 35 °C in the presence of increasing salt concentration (in mM, indicated in the figure). The curves, presented in a monolog-scale, were shifted for clarity. The arrows in b) indicate the IP peak at 2 mM NaCl and emergent Bragg peaks at 250 and 500 mM NaCl.

shows SAXS curves obtained in the presence of increasing salt concentration at 15 °C (gel — most probably a kind of ripple gel since it is above the DSC pre-transition shown in Riske et al. [13]), 25 °C (IP and fluid) and 35 °C (fluid). All curves show a broad bilayer peak, around $q=0.12$ Å^{-1}, arising from the electron density contrast between the bilayer and the solvent. This bilayer peak changes slightly with temperature, as previously analyzed [13]. As shown in an earlier work [16], a peak around $q_1=0.017$ Å^{-1} was detected only in the IP phase (with 2 mM salt). As presented in the current work, such a characteristic IP peak is detected at 25 °C only up to 10 mM NaCl (see Fig. 1b). Fig. 2 shows the low scattering angle region in detail. The IP peak is well-pronounced in the absence of salt, and becomes progressively broader upon salt addition. It is still detected in the presence of 10 mM NaCl, but it is clearly absent with 20 mM NaCl, when the overall curve profile evidently changes. Up to 10 mM NaCl there is a decrease in intensity at lower q values, evidencing interference associated with the IP peak, whereas the 20 mM sample shows a marked increase in the low q intensity, returning to the q^{-2} behavior observed for the gel and fluid phases. Similar to what has been reported before [16], no peak at q_1 was detected outside the IP, in the gel and fluid phases (see data between 2 and 10 mM NaCl in Fig. 1a and c). A more detailed study of the vanishing of the IP with salt with several other techniques will appear in a forthcoming paper and will not be discussed here.

In the gel (Fig. 1a) and fluid phases (Fig. 1b for 20–500 mM NaCl and Fig. 1c), the single broad bilayer peak is the main feature up to 100 mM NaCl, showing that DMPG is organized mainly in uncorrelated bilayers. The bilayer peak region did not show detectable changes with the increase in ionic strength in this range. The data in both gel and fluid phases could be all well-fit with the step-model discussed in the Materials and methods, giving similar structural parameters to those obtained

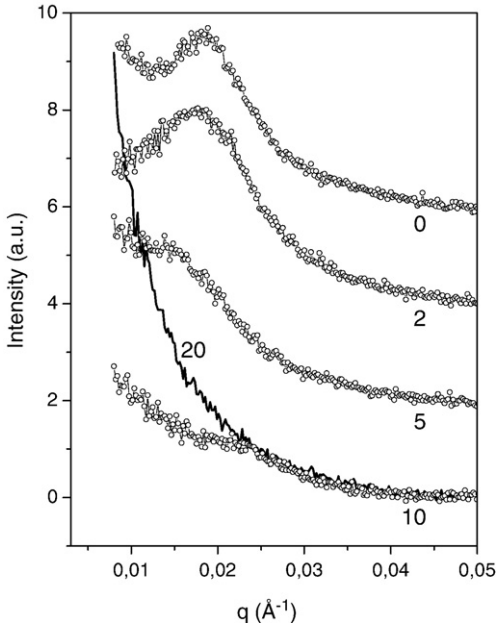

Fig. 2. Detail of the low angle region of SAXS curves of 50 mM DMPG in 10 mM Hepes pH 7.5 at 25 °C in the presence of 0, 2, 5, 10 (connected symbols) and 20 mM NaCl (line) (same data as shown in Fig. 1). For clarity, the data obtained with 0, 2 and 5 were shifted by 6, 4 and 2 units of intensity, respectively.

previously with 2 mM NaCl in the same phases [13,16]. The presence of salt does not change appreciably the electron density in the polar head region since the sodium has volume and electron density similar to those of a water molecule.

At high salt concentrations (250 and 500 mM NaCl) a clear emergent Bragg peak, characteristic of a multilamellar array, is superimposed to the bilayer form factor in both gel and fluid phases (see Fig. 1). This shows that the charge screening sets off the stabilization of a definite interlayer distance. This is more evident for the 500 mM NaCl condition in the fluid phase, where both first and second order peaks are perceptible (see arrows in Fig. 1b), though the dominant feature is still the bilayer form factor. Similar behavior was found with dispersions of 130 mM DPPG, for which a prevailing Bragg peak was not detected until 700 mM NaCl [10].

In the region 100–250 mM NaCl there is already some evidence of interference in the curve at low q values. However, only above 250 mM NaCl the correlation builds up a clear sign of a Bragg peak superimposed to the bilayer peak.

It should be remarked that, although the SAXS curve with high salt is very characteristic, the exact amount of salt at which the changes appear is very sensitive to the particular DMPG stock and sample preparation conditions. In a previous work [22], the SAXS curves with defined interference appeared already with 100 mM NaCl, and the type of curve here obtained only with 500 mM NaCl was there obtained already with 250 mM NaCl. Such result could not be reproduced with DMPG from posterior stocks. So, although the interpretation of the curves with "high salt" is trustable, the amount of salt necessary to induce the "high salt" response depends on the particular DMPG stock and on fine details of the sample preparation procedure. This point will be discussed again later in the paper.

In the following section we put forward a model that includes a structure factor $S(q)$ superimposed to the bilayer form factor $F(q)$ shown in the Materials and methods to fit the experimental curves of DMPG at very high ionic strength.

3.2. Analysis of the SAXS curves of high ionic strength DMPG

In order to understand the formation of the diffraction peaks at high salt, it is necessary to model the interference function. The curves in the presence of 250–500 mM NaCl in Fig. 1 evidence that the form factor is still clearly manifested, so the interference function does not reach zeros between the Bragg peaks, as occurs in a true lamellar phase.

Vesicles with multibilayers have been often analyzed using crystalline models. Bouwstra et al. [23] used a polycrystalline approach, with a sum of scattering terms due to structures with N lamellae, but this approach leads to a high percentage of unilamellar vesicles to account for the high intensity between the Bragg peaks. More recently, Pabst et al. [24,25] used a more sophisticated approach, taking into account the decay in order due to defects in 1-D crystals, such as thermal disorder, stacking faults (paracrystalline theory) and bending fluctuations (modified Caillé theory). When the type of disorder is known a priori, the approach used in Pabst et al. [24] is able to give electron density profiles from a global fitting procedure [24]. Furthermore, such theory should be used when the power-law diffuse scattering under the Bragg peaks is detectable and the analysis is focused on membrane fluctuations, which is not our case. On the other hand, information on the bilayer correlation length has frequently been obtained directly from the linewidth of a Lorentzian shaped quasi-Bragg peak [26,27]. We shall use this approach, which is a sufficient approximation in our case.

We are studying a dilute system with charged phospholipids not completely screened, for which the water interbilayer thickness is much larger than in neutral phospholipids. In such conditions, besides the type of defects considered in the crystalline models, there is also the possibility of eventual loss of parallelism between bilayers as a function of a not well-defined water thickness.

Our model has also the inclusion of an additional term in the scattered intensity, as proposed by Pabst et al. [24]. So, instead of Eq. (1) the relation to be used should be:

$$I(q)\left(\frac{N}{q^2}\right)\cdot[F(q)]^2\cdot[S(q)+N_{\mathrm{d}}] \tag{4}$$

where N_{d} is a scaling constant for the additional diffuse scattering term, due to positionally uncorrelated bilayers. It should be stressed that Eq. (4) is not intended to represent a defined mixture of unilamellar and multilamellar vesicles. The N_{d} term in Eq. (4) shall be interpreted as coming from bilayers that are beyond the correlation length, and therefore not correlated. In a true crystal $N_{\mathrm{d}}=0$ and in a true liquid $N_{\mathrm{d}}=1$ since the correlation function tends to be 1 at large distances.

This choice allows the introduction of a simple $S(q)$ interference function, corresponding to a sum of Lorentzian functions, given by:

$$S(q)=\sum_i f_i\cdot\left[\frac{1}{\pi}\cdot\frac{\gamma_i/2}{(\gamma_i/2)^2+(q-q_i)^2}\right] \tag{5}$$

with a defined position q_i and width at half maximum intensity γ_i for each observed peak. The Lorentzian function is the Fourier transform of a correlation function decaying with distance in the real space with a characteristic correlation length ξ, which is related to the inverse of the Lorentzian linewidth.

A good fit to experimental curves by such procedure justifies this approach. It should be stressed that a Lorentzian broadening corresponding to N lamellar distances does not mean that vesicles have N shells; it just means that the positional correlation is lost after N lamellar distances. Thus it can either indicate that we have oligolamellar structures with N lamellae or loose multilamellar vesicles (with $N\gg1$). An idea about the preferred structure is however obtained by visualization with optical microscopy, as discussed later on.

We have fit the data obtained with 50 mM DMPG in 250 and 500 mM NaCl at temperatures between 15 and 35 °C, thus covering the gel and fluid phases, using the sum of two Lorentzians. The sub-index i in Eq. (5) represents the diffraction order. We have imposed that $q_1=q_2/2=q_{\mathrm{d}}$, because this is expected for first and second orders coming from the same lamellar pattern. Fig. 3 shows the experimental curves with fit curves and the correspondent $F(q)$ and $S(q)$ for DMPG in 500 mM NaCl at 15 °C

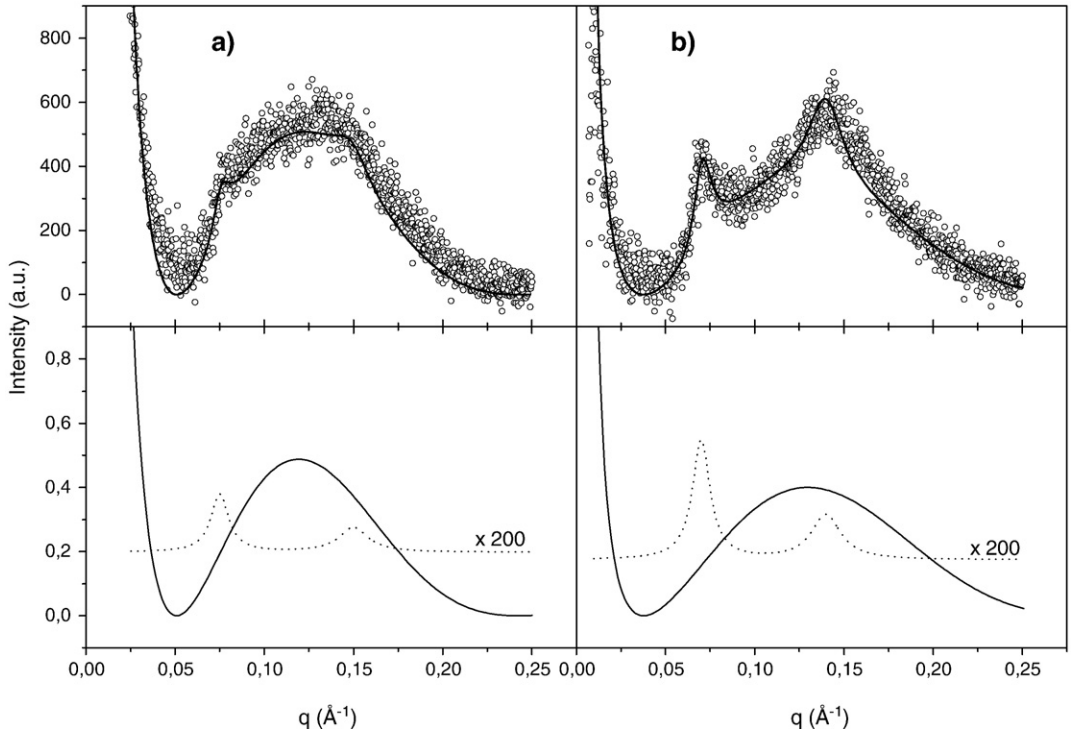

Fig. 3. Top — Experimental (points) and fitting (bold lines) curves of 50 mM DMPG in 10 mM Hepes pH 7.4 in the presence of 500 mM NaCl at a) 15 °C and b) 25 °C. Bottom — The correspondent form factor $F(q)$ (line) and structure factor $S(q)$ (dots) of the fits shown on top for a) 15 °C and b) 25 °C. The $S(q)$ curves were multiplied by 200, so they could be visualized in the same scale. The structural fitting parameters are shown in Table 1.

(gel) and 25 °C (fluid). The bilayer form factor $F(q)$ was kept constant during the fitting procedure, to reduce the number of free parameters. The same structural parameters that could fit the bilayer peak at lower ionic strengths in the gel and fluid phases were used (see Table 1). Table 1 shows the fitting parameters used to fit all curves analyzed with 500 mM NaCl.

Table 1
Structural parameters used to fit the experimental curves (50 mM DMPG in 500 mM NaCl) using Eq. (4), where $F(q)$ is given in Eq. (3) and $S(q)$ in Eq. (5)

$S(q)$					$F(q)$						
Temp	N_d	f_1	f_2	q_d	R_1	R_2	R_3	d_b	ρ_1	ρ_2	ρ_3
15 °C	0.99	0.013	0.010	0.075							
20 °C	0.99	0.013	0.010	0.075	10	12.5	3.5	52	0.44	0.32	0.21
25 °C	0.87	0.033	0.025	0.070							
30 °C	0.87	0.025	0.022	0.072	10	8.9	3.5	44.8	0.435	0.29	0.19
35 °C	0.87	0.021	0.019	0.073							
40 °C	0.87	0.026	0.024	0.074							

The thicknesses are given in Å, q_d in $Å^{-1}$ and the electron densities in e/$Å^3$. The same normalization constant was used for all temperatures to ensure the same number of scattering units. The bilayer form factor was kept constant at reasonable values for the gel (below T_m=23 °C) and fluid (above T_m=23 °C) phases [13,16]. The same Lorentzian linewidths were used for all curves, to reduce the number of free parameters: γ_1=0.006 $Å^{-1}$, γ_2=0.012 $Å^{-1}$. These values were chosen for temperatures where the peak widths could be directly measured from the experimental data. N_d, q_d, f_1 and f_2 were left free, except at 15 and 20 °C, when we imposed that $f_1 > f_2$. The acyl chain density ρ_2 in the gel phase was kept constant at 0.32 e/$Å^3$. The fits were done with density contrasts in respect to water, with ρ_w=0.33 e/$Å^3$. T is the bilayer thickness given by d_b=2(R_1+R_2+R_3). The errors estimated during the fitting procedure, while keeping the parameters within reasonable physical constraints, were generally less than 5%. Larger errors (15%) were obtained for the Lorentzian intensities f_1 and f_2.

The structure factor used to fit the data yielded reasonable fits and consistent structural parameters. The fact that N_d is higher and f_1 and f_2 are smaller in the gel ripple phase than in the fluid phase, indicates that lamellae are less ordered, possibly because the ripples in the bilayer cause a fluctuation in the interbilayer distance. In fact, the Bragg peak is much less pronounced at 15 than at 25 °C. The incipient lamellar repeat distance d can be calculated from the first order peak position ($d=2\pi/q_d$) and is shown as a function of temperature in Fig. 4. The increase in the repeat distance at T_m might indicate an increase in the water layer among lamellae, since the bilayer thickness decreases at T_m. This can be explained by an increase in interlayer repulsion due to changes in counterion binding to the bilayer surface. The lamellar repeat distances obtained here for DMPG in the gel and fluid phases are very similar to those obtained with 130 mM DPPG [10] in the presence of 500 mM NaCl.

From the Lorentzian linewidth we are able to estimate a typical correlation length $\xi=2/\gamma$ for 50 mM DMPG in 500 mM NaCl. The fits were done fixing γ_1=0.006 $Å^{-1}$, which could be directly measured from the linewidth at half maximum of the first order peak obtained in the fluid phase (see Fig. 2b). The experimental resolution of the set-up in the peak region is 0.001 $Å^{-1}$, so that its effect in the linewidth is negligible. In the gel phase, γ_1 could not be measured and the same value was used for the fits. Thus, for the fluid phase we can estimate $\xi \sim 330$ Å, which corresponds to $\sim 4d$, meaning that, on average, four lamellae are positionally correlated.

Similar fits were obtained with 250 mM NaCl between 15 and 35 °C (not shown), although the Bragg peaks were less pronounced than with 500 mM NaCl (see Fig. 1). The peak at

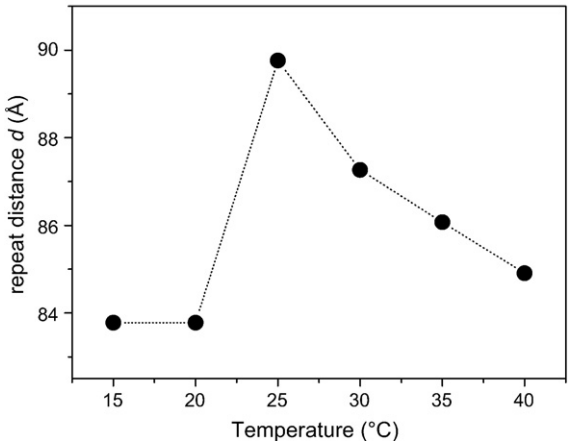

Fig. 4. Temperature dependence of the lamellar repeat distance $d=2p/q_d$ (Table 1) for 50 mM DMPG in 500 mM NaCl.

$q=0.128$ Å^{-1} is most likely a second order peak, the first one coinciding with a zero of the form factor. This would correspond to a lamellar repeat distance of $d=97$ Å, higher than with 500 mM NaCl, as expected due to a higher interlayer repulsion.

3.3. Effect of sample preparation

Below 100 mM NaCl, DMPG dispersions form preferentially unilamellar vesicles or uncorrelated lamellae, although some incipient correlation can already be perceived with 100 mM NaCl in this study and existed clearly already in a previous study with other DMPG stock [22]. To better understand the action of salt in the transformation of unilamellar into multilamellar structures, we tested the effect of adding 500 mM NaCl to a low salt dispersion of DMPG, for which only the form factor was present (as the curve with 2 mM NaCl in Fig. 1). The later addition of salt did not change the scattering curve, as shown in Fig. 5, showing that once formed, the vesicles do not break and rearrange into multilamellar structures within the timescale of one day. The multilamellar vesicles are formed only when the lipid film is dispersed in a buffer that already contains salt. This was expected, because transformation of unilamellar into multilamellar vesicles requires a complete reorganization of the bilayers. Thus, we can also conclude that at low ionic strength, DMPG is most probably organized in unilamellar vesicles.

3.4. Optical microscopy

Fig. 6 shows pictures of DMPG dispersions obtained with optical microscopy. Even though individual vesicles can be distinguished only when their sizes are on the micrometer range, general sample appearance can be assessed with optical microscopy. Up to 20 mM NaCl, only submicroscopic structures, most probably vesicles, which diffused throughout the whole observation chamber, were observed in the gel and fluid phases, similar to what has been previously reported for DMPG at lower ionic strengths [16]. These vesicles are most probably unilamellar, as their SAXS data indicate no correlation whatsoever and their sizes are small. In the presence of 50–250 mM NaCl, giant multilamellar vesicles (MLVs) with diameters around 10 μm were seen deposited at the bottom of the chamber, although submicroscopic vesicles were still observed diffusing everywhere inside the chamber (see the difference between snapshots taken with the focus set at the bottom of the chamber and above it, marked as top, in Fig. 6). Although a single MLV can accommodate a huge amount of lipids, there were far more small vesicles inside the chamber. A very rough estimate taking into account the lipid concentration, the chamber size and the density of MLVs deposited at the bottom, shows that most of the lipids are still forming submicroscopic vesicles up to 100 mM NaCl. With 500 mM NaCl, however, mainly MLVs at the bottom were seen (Fig. 6 bottom), and no relevant population of submicroscopic vesicles could be found (Fig. 6 top). Thus, upon progressive salt addition, more MLVs and less submicroscopic vesicles are formed. Furthermore, the optical density of the individual MLVs increases with salt, showing that the number of lamellae per vesicle also increases.

From the SAXS data, a clear signal of positionally correlated lamellae was detected only above 250 mM NaCl. Formation of large MLVs does not imply that their lamellae should be positionally well correlated. In fact, some authors mention an unbound multilamellar vesicle state for mixtures of PG and phosphatidylethanolamine [25,28]. Careful observation of many MLVs formed in the presence of 50–100 mM NaCl even show uncorrelated lamellae in their outskirts, as indicated with asterisks in Fig. 7. Such structures were not observed at higher salt concentrations. The optical contrast of these loose structures indicates that they in fact consist of single bilayers.

In the presence of 500 mM NaCl, lipids are engaged in forming predominantly dense multilamellar structures, as seen with optical microscopy (Fig. 6). However, analysis of the SAXS data show that correlation distance among lamellae lasts only about 330 Å in the fluid phase, corresponding to roughly 4 lamellae. Thus, although MLVs are clearly detected with this very high ionic strength, and is the prevailing structure seen, the correlation among the bilayers is loose. Furthermore, it becomes clear that oligolamellae with ~4 lamellae are not the preferred

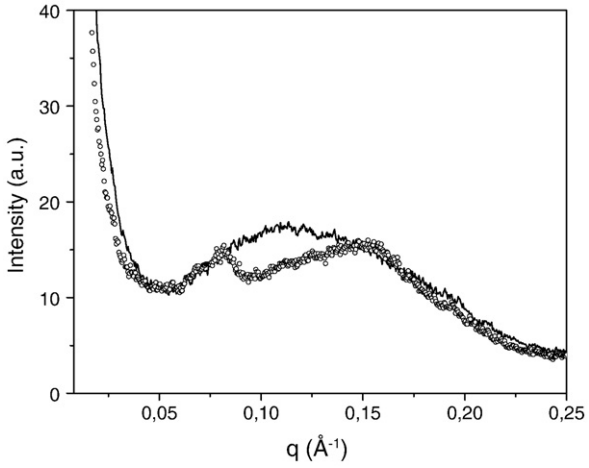

Fig. 5. SAXS data of 50 mM DMPG in the presence of 500 mM NaCl obtained in two different ways: dispersions prepared with salt (points) and dispersions prepared without salt with later addition of salt (line).

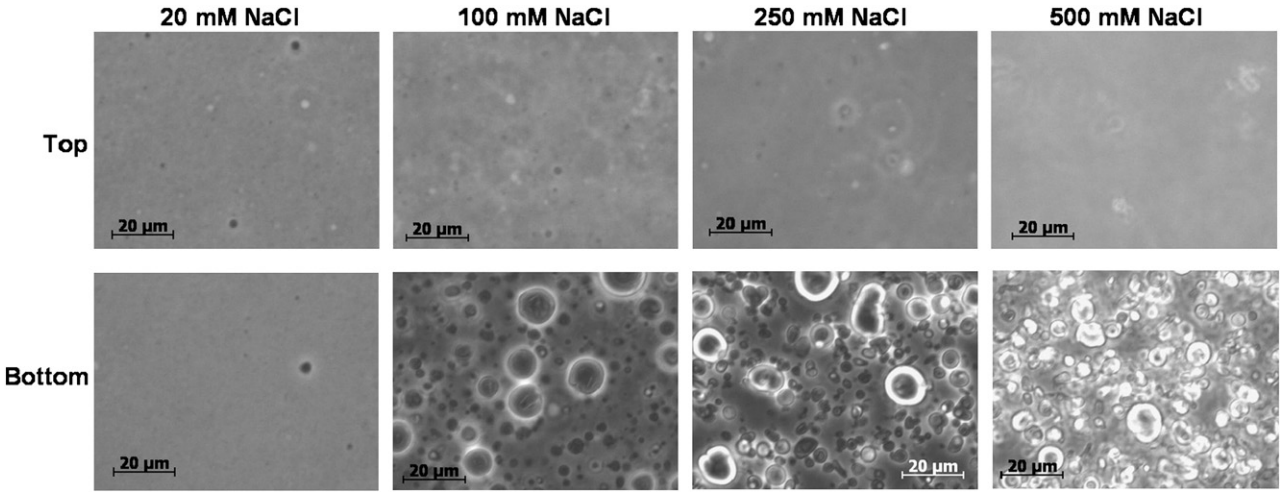

Fig. 6. Phase contrast images of DMPG dispersions prepared at 50 mM DMPG with different amounts of salt (indicated on top) and then diluted to 2.5 mM DMPG (20 mM NaCl; 17 °C) and 0.7 mM DMPG (100–500 mM NaCl; room temperature) to reduce sample turbidity and allow optical observation. As in the case of later salt addition (previous section), we expect that structures already formed will not change upon dilution. The snapshots marked with Top were obtained inside the chamber, above the cover slit surface, whereas those marked with Bottom were taken with the focal plane slightly above the cover slit. The snapshots of the MLVs were taken with the same illumination, so differences in vesicle optical contrast could be qualitatively evaluated. Pictures obtained with 50 mM NaCl were very similar to those with 100 mM NaCl, but they are not shown as they were not taken in the exact same conditions of the series 100–500 mM NaCl.

structures formed by DMPG at this ionic strength. The incipient Bragg peaks observed in the SAXS curves come from loosely correlated multilamellar vesicles. Further salt addition would certainly increase the lamellar order, as is the case of DPPG dispersions [10].

It is interesting to compare the characteristics of dispersions of DMPG with 500 mM NaCl and DMPC, which share an almost identical thermal behavior. Observation of DMPC dispersions under a microscope also reveals the predominance of MLVs with ~10 µm diameter and the absence of small vesicles (Fig. 8), very similar to DMPG with 500 mM NaCl (Fig. 6). However, SAXS data clearly show that DMPG lamellae are further apart and their correlation is loose, whereas clear Bragg peaks arise from DMPC dispersions [14]. We want here to call the attention to the combination of optical microscopy observation of lipid dispersions with other conventional techniques, such as SAXS, which definitely enriches the study of lipid dispersions.

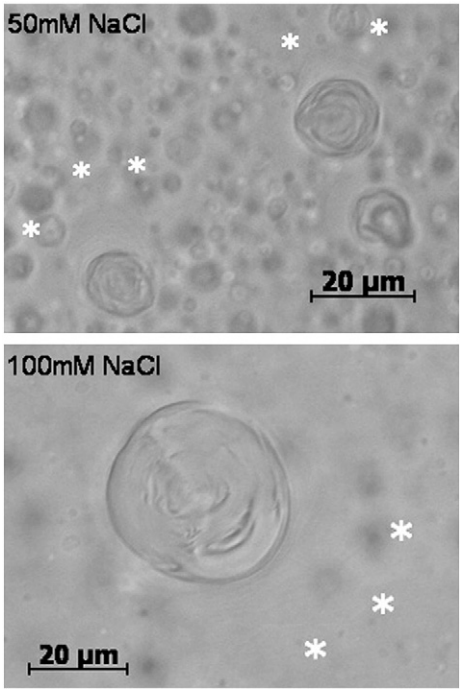

Fig. 7. Bright field microscopy image of DMPG dispersions prepared at 50 mM DMPG with 50 and 100 mM NaCl and further diluted to 0.7 mM DMPG. Asterisks indicate the end of the loose lamellar structure.

3.5. Interaction between charged surfaces: DLVO theory

A definite water layer between lipid bilayers is established when repulsive and attractive forces balance, forming an energy interaction minimum. Van der Waals interaction is always attractive, whereas electrostatic interaction between charged surfaces and hydration and steric forces are repulsive [29]. The DLVO theory was developed in the 1940s to describe colloidal stability and takes into account the repulsive double-layer interaction and the van der Waals attraction between charged surfaces/particles (see for instance [30]). Hydration forces can be neglected at a first approximation when dealing with charged

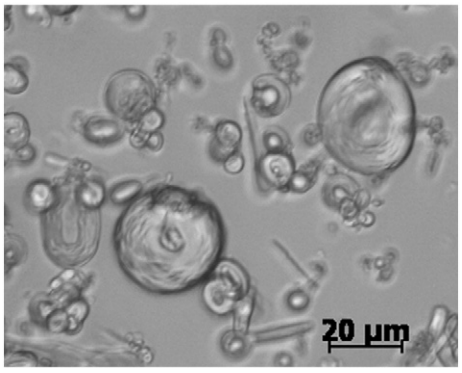

Fig. 8. Bright field microscopy image of 1 mM DMPC dispersions.

Table 2
DMPG surface potential Ψ_o and Debye length $1/\kappa$ calculated for different amounts of added salt (the ionic strength of the Hepes buffer, 4 mM, was added to all conditions)

[NaCl], mM	Ψ_o (mV)	$1/\kappa$ (Å)
2	−160	40
10	−146	26
50	−104	13
100	−86	10
250	−62	6.1
500	−44	4.3
700	−35	3.6
1000	−26	3.1

Ψ_o was calculated using the Gouy–Chapmann theory and assuming a Na^+–PG^- binding constant of $K_{Na}=0.3\ M^{-1}$ [32]. $T=303$ K.

surfaces, since these forces play a role mainly at short distances (below 20 Å; [31]). The interaction energy $W(D)$ between two charged surfaces can thus be estimated using the DLVO theory as a function of the medium ionic strength and the surface charge density. At low ionic strength and/or high surface potential, the double-layer repulsion dominates and no minimum in the interaction energy exists. Yet, an energy minimum can be obtained at high ionic strength and/or low surface potential. Only in this situation a multilamellar structure of charged lipids can be stable.

We have used here the DLVO theory to estimate the interaction energy $W(D)$ per unit area between charged surfaces separated by a distance D as a function of the ionic strength n. The interaction energy $W(D)$ can be written as [30]:

$$W(D) = \left(64 \times 10^3 kTN_A n\gamma^2/\kappa\right)e^{-\kappa D} - A/12\pi D^2, \qquad (6)$$
$$\gamma = \tanh(ze\psi_o/4kYT)$$

where k is the Boltzmann constant, T the absolute temperature, N_A the Avogadro's number, z the electrolyte valence, $1/\kappa$ is the Debye length, Ψ_o is the surface potential and A is the Hamaker constant. The first term in Eq. (6) accounts for the double-layer repulsion, whereas the second term consists of the van der Waals attraction between two infinite planar surfaces. The Debye length depends on the medium ionic strength, and sets the typical diffuse ionic double-layer thickness near a charged surface. The surface potential Ψ_o can be estimated using the Gouy–Chapmann theory (see for instance [30]), with an additional contribution of a small binding constant between sodium ions and PG headgroups [32]. Table 2 shows the Debye length and surface potential calculated for different ionic strengths.

The interaction energy between charged surfaces was then calculated inserting the values listed in Table 2 into Eq. (6). For the Hamaker constant, we used $A=2\times10^{-21}$ J, which was previously calculated for PG in 100 mM NaCl [33]. The curves $W(D)$ obtained are shown in Fig. 9.

We see in Fig. 9 that the interaction energy is always positive when the ionic strength is lower than 100 mM NaCl, and no minimum is formed. This means that no stable distance between bilayers arises. Accordingly, our SAXS and optical microscopy data show that up to 100 mM NaCl, DMPG is arranged mainly in uncorrelated bilayers. At very low ionic strength, the electrostatic repulsion is active even beyond 100 Å. Above 100 mM NaCl, negative W values exist and a minimum starts to build for distances around tens of Å. For 250 and 500 mM NaCl this minimum is still shallow and not very well-defined. From our SAXS data, the lamellar repeat distances found for these two conditions were $d=97$ and 87 Å, respectively (at 30 °C, fluid phase). If we assume that the bilayer thickness is 45 Å (see Table 1), we find an interlayer distance of 52 and 42 Å, respectively. Thus, the position of the shallow minima predicted by the DLVO theory coincides pretty well with the estimated water layer between the loosely correlated lamellae obtained from SAXS data (see the asterisks in Fig. 9). The fact that the minimum in W observed for 250–500 mM NaCl is not well-defined and shallow indicates that the correlation among the layers is still loose and is consistent with the results obtained from the SAXS modeling that the positional order is lost after ~4d. Interestingly, Degovics et al. [10] found for DPPG that a clear Bragg pattern appeared only above 700 mM NaCl. From

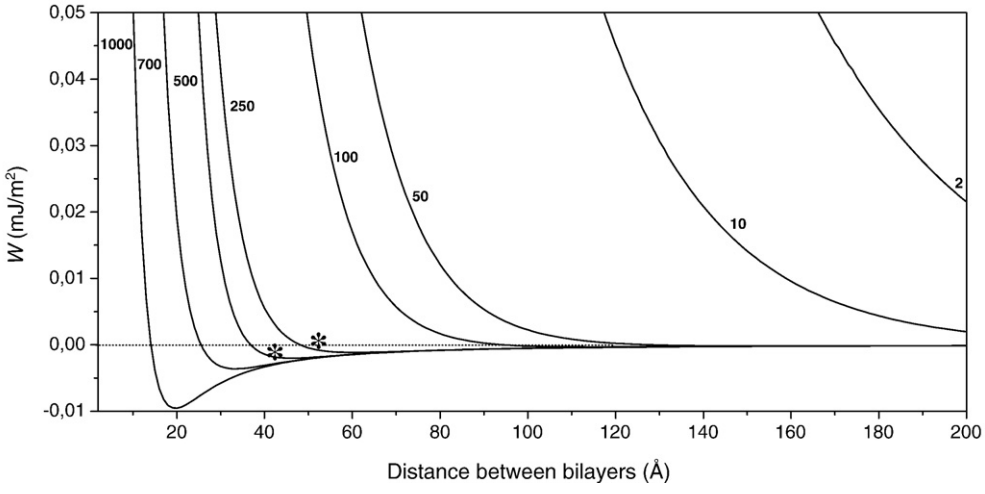

Fig. 9. Interaction energy per unit area W as a function of the distance between the bilayers for different ionic strengths (shown in the figure in mM). The asterisks show the typical water layer distance found in the SAXS experiments for DMPG in the presence of 250 and 500 mM NaCl.

the estimation done with the DLVO theory, the minimum in W gets indeed more defined above this salt concentration. A really well-defined energy minimum at $D=20$ Å is shaped only in the presence of 1 M NaCl.

In summary, the predictions done with the DLVO theory can explain remarkably well the formation of multilamellar structures with DMPG/DPPG bilayers with the increase in the ionic strength. Thus, multibilayers are formed when the ionic strength is high enough to screen the double-layer repulsion, so that a balance between van der Waals attraction and electrostatic repulsion is established. There was no need to take into account hydration forces to explain the experimental results. Indeed, these are relevant only below 20 Å, and might play a role above 1 M NaCl.

4. Conclusions

In this work we have investigated the effect of salt on the structure of DMPG dispersions with SAXS and optical microscopy. We could establish that at 25 °C the IP persists only up to 10 mM NaCl. Between 2 and 100 mM NaCl in both gel and fluid phases, a single bilayer scattering peak was observed and mainly submicroscopic vesicles were seen with optical microscopy. Therefore, similar to other charged lipids, DMPG dispersions at relatively low ionic strengths spontaneously form submicroscopic unilamellar vesicles. In fact, no stable distance exists according to the DLVO theory due to the high bilayer repulsion up to 100 mM salt. In the presence of 250–500 mM NaCl, incipient Bragg peaks, characteristic of lamellar repeat distances $d\sim 90$–100 Å, were detected superimposed to the bilayer form factor. A prevailing multilamellar pattern similar to the one of DMPC was not observed. Mainly giant multilamellar vesicles were seen with optical microscopy (500 mM NaCl). Fitting of the SAXS data revealed that around 4 lamellae are positionally correlated within these loose multilamellar structures. Thus, this early positional order is much less defined than the lamellar stacking of true lamellar systems (e.g. lecithins) and resembles that found in liquids. The DLVO theory showed that a first energy minimum was shaped, in fact, only around 250 mM NaCl. The interbilayer distances predicted with the DLVO theory agreed very well with those estimated from the SAXS data (250–500 mM NaCl). The energy minimum was still shallow and not well-defined, explaining why the multilamellar structure was loose. A well-shaped minimum was achieved only with 1 M NaCl, when a more conventional multilamellar structure might form.

Under physiological conditions ($\sim$150 mM salt), DMPG presents a very similar thermal behavior to DMPC, but its swelling abilities, as evidenced by the much larger water thickness between bilayers, are still rather different, which might be of biological relevance.

Acknowledgements

We thank the LNLS (Laboratório Nacional de Luz Síncrotron) staff. Evandro Luis Duarte helped in some measurements. This work was supported by FAPESP, CNPq.

References

[1] J.F. Nagle, S. Tristram-Nagle, Structure of lipid bilayers, Biochim. Biophys. Acta 1469 (2000) 159–195.
[2] J. Seelig, P.M. MacDonald, P.G. Scherer, Phospholipid head groups as sensors of electric charges in membranes, Biochemistry 26 (1987) 7535–7541.
[3] T. Heimburg, R.L. Biltonen, Thermotropic behavior of dimyristoyl phosphatidylglycerol and its interaction with cytochrome *c*, Biochemistry 33 (1994) 9477–9488.
[4] M.H. Biaggi, K.A. Riske, M.T. Lamy-Freund, Melanotropic peptides–lipid bilayer interaction. Comparison of the hormone α-MSH to a biologically more potent analog, Biophys. Chem. 67 (1997) 139–149.
[5] R.M. Fernandez, M.T. Lamy-Freund, Correlation between the effects of a cationic peptide on the hydration and fluidity of anionic lipid bilayers: a comparative study with sodium ions and cholesterol, Biophys. Chem. 87 (2000) 87–102.
[6] R.P. Rand, V.A. Parsegian, Hydration forces between phospholipid bilayers, Biochim. Biophys. Acta 988 (1989) 351–376.
[7] H. Hauser, F. Paltauf, G.G. Shipley, Structure and thermotropic behavior of phosphatidylserine bilayer membranes, Biochemistry 21 (1982) 1061–1067.
[8] M. Kodama, T. Miyata, Effect of Na^+ concentrations on both size and multiplicity of multilamellar vesicles composed of negatively charged phospholipid as revealed by differential scanning calorimetry and electron microscopy, Thermochim. Acta 267 (1995) 365–372.
[9] M.M.A.E. Claessens, B.F. van Oort, F.A.M. Leermakers, F.A. Hoekstra, M.A.C. Stuart, Charged lipid vesicles: effects of salts on bending rigidity, stability, and size, Biophys. J. 87 (2004) 3882–3893.
[10] G. Degovics, A. Latal, K. Lohner, X-ray study on aqueous dispersions of dipalmitoyl phosphatidylglycerol in the presence of salt, J. Appl. Crystallogr. 33 (2000) 544–547.
[11] I.S. Salonen, K.K. Eklund, J.A. Virtanen, P.K.J. Kinnunen, Comparison of the effects of NaCl on the thermotropic behavior of *sn*-1′ and *sn*-3′ stereoisomers of 1,2-dimyristoyl-*sn*-glycero-3-phosphatidylglycerol, Biochim. Biophys. Acta 982 (1989) 205–215.
[12] K.A. Riske, M.J. Politi, W.F. Reed, M.T. Lamy-Freund, Temperature and ionic strength dependent light scattering of DMPG dispersions, Chem. Phys. Lipids 89 (1997) 31–44.
[13] K.A. Riske, L.Q. Amaral, M.T. Lamy-Freund, Thermal transitions of DMPG bilayers in aqueous solution: SAXS structural studies, Biochim. Biophys. Acta 1511 (2001) 297–308.
[14] M.T. Lamy-Freund, K.A. Riske, The peculiar thermo-structural behavior of the anionic lipid DMPG, Chem. Phys. Lipids 122 (2003) 19–32.
[15] M.F. Schneider, D. Marsh, W. Jahn, B. Kloesgen, T. Heimburg, Network formation of lipid membranes: triggering structural transitions by chain melting, Proc. Natl. Acad. Sci. U. S. A. 96 (1999) 14312–14317.
[16] K.A. Riske, L.Q. Amaral, H.-G. Döbereiner, M.T. Lamy, Mesoscopic structure in the chain-melting regime of anionic phospholipid vesicles: DMPG, Biophys. J. 86 (2004) 3722–3733.
[17] K.A. Riske, H.-G. Döbereiner, M.T. Lamy, Gel–fluid transition in diluted versus concentrated DMPG aqueous dispersions, J. Phys. Chem., B 106 (2002) 239–246.
[18] G. Cevc, A. Watts, D. Marsh, Non-electrostatic contribution to the titration of the ordered-fluid phase transition of phosphatidylglycerol bilayers, FEBS Lett. 120 (1980) 267–270.
[19] H.-G. Döbereiner, Properties of giant vesicles, Curr. Opin. Colloid. Interface Sci. 5 (2000) 256–263.
[20] R. Dimova, S. Aranda, N. Bezlyepkina, V. Nikolov, K.A. Riske, R. Lipowsky, A practical guide to giant vesicles. Probing the membrane nanoregime via optical microscopy, J. Phys.: Condensed Matter 18 (2006) 1151–1176.
[21] O. Glatter, O. Kratky, Small Angle X-ray Scattering, Academic Press, New York, 1982.
[22] K.A. Riske, Ph.D. thesis, Institute of Physics, University of Sao Paulo, Sao Paulo, 2001.

[23] J.A. Bouwstra, G.S. Gooris, W. Bras, H. Talsma, Small angle X-ray scattering: possibilities and limitations in characterization of vesicles, Chem. Phys. Lipids 64 (1993) 83–98.
[24] G. Pabst, R. Koschuch, B. Pozo-Navas, M. Rappolt, K. Lohner, P. Laggner, Structural analysis of weakly ordered membrane stacks, J. Appl. Crystallogr. 36 (2003) 1378–1388.
[25] B. Pozo-Navas, K. Lohner, G. Deutsch, E. Sevcsik, K.A. Riske, R. Dimova, P. Garidel, G. Pabst, Composition dependence of vesicle morphology and mixing properties in a bacterial model membrane system, Biochim. Biophys. Acta 1716 (2005) 40–48.
[26] A. Bóta, M. Kriechbaum, Prehistory in the pretransition range of dipalmitoylphosphatidylcholine/water system, Colloids Surf., A 141 (1998) 441–448.
[27] J.M. Holopainen, J. Lemmich, F. Richter, O.G. Mouritsen, G. Rapp, P.K.J. Kinnunen, Dimyristoylphosphatidylcholine/C16:0-ceramide binary liposomes studied by differential scanning calorimetry and wide- and small-angle X-ray scattering, Biophys. J. 78 (2000) 2459–2469.
[28] B. Pozo-Navas, V.A. Raghunathan, J. Katsaras, M. Rappolt, K. Lohner, G. Pabst, Discontinuous unbinding of lipid multibilayers, Phys. Rev. Lett. 91 (2003) 28101–1–28101-4.
[29] J.N. Israelachvili, Intermolecular and Surfaces Forces, Academic Press, San Diego, 1991.
[30] P.C. Hiemenz, Principles of Colloids and Surface Chemistry, Marcel Dekker, New York, 1986.
[31] T. McIntosh, S.A. Simon, Hydration and steric pressures between phospholipids bilayers, Annu. Rev. Biophys. Biomol. Struct. 23 (1994) 27–51.
[32] K.A. Riske, O.R. Nascimento, M. Peric, B.L. Bales, M.T. Lamy-Freund, Probing DMPG vesicle surface with a cationic aqueous soluble spin label, Biochim. Biophys. Acta 1418 (1999) 133–146.
[33] M.E. Loosley-Millman, R.P. Rand, V.A. Parsegian, Effects of monovalent ion binding and screening on measured electrostatic forces between charged phospholipids bilayers, Biophys. J. 40 (1982) 221–232.